ELSEVIER

Journal of Power Sources 97–98 (2001) 247–250

JOURNAL OF POWER SOURCES

www.elsevier.com/locate/jpowsour

Electrochemical performance of $Pb_3(PO_4)_2$ anodes in rechargeable lithium batteries

Zhaolin Liu[a,*], Jim Yang Lee[b]

[a]*Institute of Materials Research and Engineering, 3 Research Link, Singapore 117602, Singapore*
[b]*Department of Chemical and Environmental Engineering, National University of Singapore, 10 Kent Ridge Crescent, Singapore 119260, Singapore*

Received 2 June 2000; received in revised form 17 November 2000; accepted 4 December 2000

Abstract

Lead phosphate was used as an intrinsic phosphorous-doped lead composite oxide in rechargeable lithium test batteries. For comparison the amorphous polymorph was prepared from the crystalline form by melt-quenching. The experimental results are analogous to tin composite oxide (TCO) anodes, with the amorphous form showing a higher capacity and better cyclability. The mechanism for rechargeability and the cause for capacity loss in the first cycle are also proposed. © 2001 Elsevier Science B.V. All rights reserved.

Keywords: Lead phosphate; Secondary lithium battery; Anode material

1. Introduction

Li-alloys such as Li–Al, Li–Sn and Li–Pb are potential anode materials for Li-ion batteries because of their high charge densities and fast room temperature Li-ion mobilities [1]. However, many reports have shown that it is difficult to realize the theoretical capacities with the alloy electrodes because of the mechanical and conductivity instabilities caused by large volume changes of the lithium storage phase during cycling. There was no real commercial interest in these alloys before Fuji's announcement of the development of lithium batteries based on amorphous tin composite oxide (TCO) negative electrodes (precursors of Li–Sn alloys) [2]. Since then, much attention has been focused on the possibility of substituting similar classes of compounds for carbon negative electrodes in Li-ion batteries. Both pristine and doped tin oxides have been extensively investigated as anode materials, but reports about lead composite oxides for Li-ion applications are relatively scarce. In this work, we consider $Pb_3(PO_4)_2$ as an intrinsic phosphorous-doped lead composite oxide and investigated the performance of its crystalline and amorphous forms as the anode materials for Li-ion batteries.

2. Experimental

2.1. Material preparations

Crystalline $Pb_3(PO_4)_2$ was purchased from Johnson Matthey and used as received. Crystalline $Pb_3(PO_4)_2$ was pelletized at 2×10^6 Pa and fired in flowing argon in a Carbolite/MTF tube furnace. After 2 h at 1020°C, the melt was removed from the furnace and quickly quenched in air between two stainless steel plates at room temperature. The vitreous solid thus, formed was carefully ground to a powder.

2.2. Composition and structure determinations

Elemental composition was determined by inductively coupled plasma spectroscopy (ICPS) on a Perkin-Elmer Optima 3000DV, using digestions of the lead composite oxides in a 1:1 (v/v) mixture of HCl/HNO_3 at 60°C. Structural characterizations by powder XRD was carried out on a Philips PW1710 diffractometer, using Cu Kα radiation ($\lambda = 1.54$ Å) and a 2θ range of 10–80°.

2.3. Cell preparation

The lead composite oxide was mixed with poly(vinylidene fluoride) (PVDF) binder (Aldrich, dissolved in advance in *n*-methylpyrrolidone) and carbon black (3M Carbon Super-P, used as conductivity enhancer) in the weight ratio

* Corresponding author. Fax: +65-8720785.
E-mail address: zl-liu@imre.org.sg (Z. Liu).

PII: S0378-7753(01)00530-4

of 80:10:10. The resulting paste was coated on round copper disks 1.6 cm in diameters, followed by drying at 120°C for 5 h and compaction at 2×10^6 Pa. Each coated disk was teamed up with a lithium counter electrode and a polypropylene separator to form a test cell. 1 M $LiPF_6$ in a 1:1 (w/w) mixture of ethylene carbonate and diethyl carbonate was the electrolyte. Cell assembly was carried out in a glove box where O_2 and H_2O contents were kept below 3 ppm each.

2.4. Electrochemical tests

All cells were tested at the constant current of 30 mA/g of active material and were charged and discharged between fixed voltage limits (0–1.4 V) on a Bitrode battery tester. Cyclic voltammetry was performed on an EG&G model 263 potentiostat/galvanostat, using the $Pb_3(PO_4)_2$ coated copper disk as the working electrode and lithium as both the counter and reference electrodes. A scan range of 0–1.6 V (versus Li^+/Li) and a scan rate of 0.1 mV/s were used. The first scan was started cathodically at around 3 V, the open-circuit voltage of most test cells.

3. Results and discussion

The composition of melt-quenched $Pb_3(PO_4)_2$ as determined by ICPS could be summarized as $Pb_3P_{1.97}O_{8.10}$. As the composition is only marginally different from that of pristine $Pb_3(PO_4)_2$ used for its preparation, decomposition of $Pb_3(PO_4)_2$ did not occur to any significant extent under the preparation conditions. Fig. 1 shows the XRD patterns of

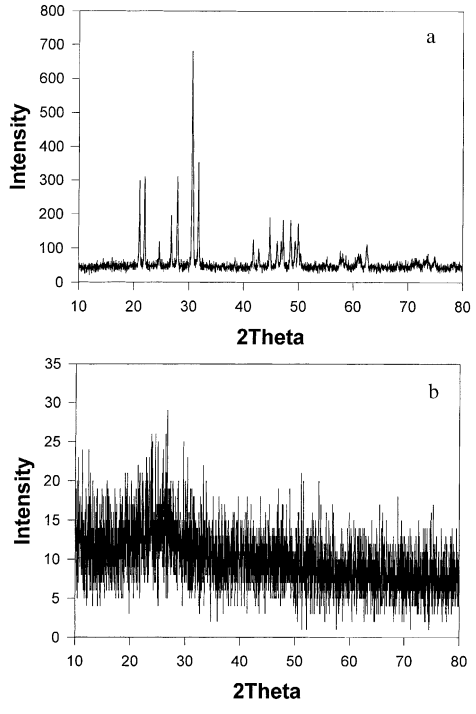

Fig. 1. XRD patterns of (a) crystalline $Pb_3(PO_4)_2$; (b) amorphous $Pb_3P_2O_8$.

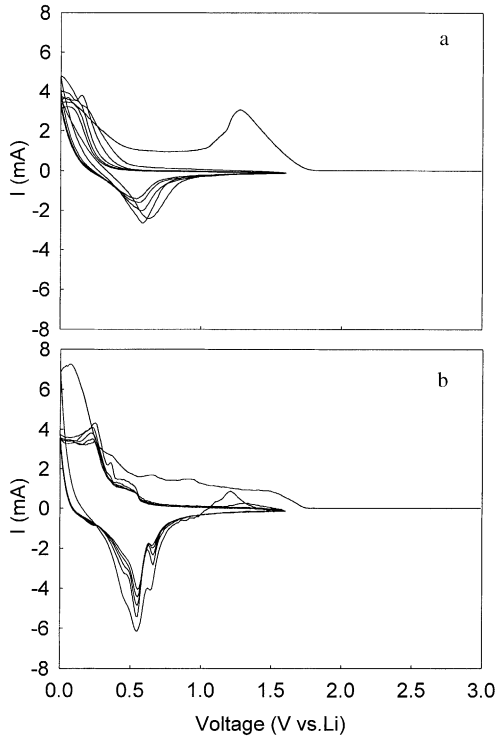

Fig. 2. Cyclic voltammograms of (a) crystalline $Pb_3(PO_4)_2$; (b) amorphous $Pb_3P_2O_8$ at 0.1 mV/s.

pristine and melt-quenched $Pb_3P_{1.97}O_{8.10}$. The powder XRD pattern of pristine $Pb_3(PO_4)_2$ is marked by several sharp diffraction peaks at 2θ values of 22, 30, and 32°. In contrast to this the melt-quenched polymorph does not give rise to any diffraction peak and the intensity of diffraction is generally low. The rapid cooling of the $Pb_3(PO_4)_2$ melt has effectively transformed the material into the vitreous form where no long-range order is observed.

There are substantial differences between the first and subsequent scans in the voltammograms of crystalline $Pb_3(PO_4)_2$ and amorphous $Pb_3P_2O_8$ (Fig. 2). In Fig. 2a, a large cathodic peak around 1.25 V appears only during the first cathodic scan. The underlying reaction is irreversible because there is no similar feature from the second scan onwards. Upon scan reversal an anodic peak emerges around 0.6 V, with diminishing peak intensity that varies with the cycle number. For amorphous $Pb_3P_2O_8$ (Fig. 2b), a large peak at 0.1 V and several smaller features around 1.6, 1 and 0.7 V may be identified in the first cathodic scan. Well-separated anodic peaks are detected at 0.55 and 0.7 V in the reverse scan, indicating that there are at least two energetically different sites for Li-ions in this polymorph. A comparison of the voltammetric features between the second and the fifth scans shows that lithium insertion/extraction reactions are more reversible in amorphous $Pb_3P_2O_8$. The electrochemical decomposition of crystalline $Pb_3(PO_4)_2$ leading to the formation of metallic Pb clusters is likely the cause for the cathodic peak around 1.25 V. It is speculated that decomposition still occurs in amorphous $Pb_3P_2O_8$

but the lead formed is too highly dispersed to contribute to an identifiable phase. If it is assumed that alloying and de-alloying are involved in reversible charge storage and retrieval [3], then the cathodic peak at 0.2 V and the anodic peak at 0.5 V are lithium insertion/extraction reactions associated with the Li–Pb alloys.

The two polymorphs of lead composite oxides were charged galvanostatically at 30 mA/g between 0 and 1.4 V (versus Li). The first cycle charge capacities for Li-ion storage were 742 and 568 mAh/g, respectively. Subsequent Li^+ extraction reactions proceeding up to 1.4 V returned discharge capacities of 296.6 for crystalline $Pb_3(PO_4)_2$ and 337.4 mAh/g for amorphous $Pb_3P_2O_8$. The corresponding first cycle Coulombic efficiencies are therefore, 40 and 59%, respectively.

Crystalline $Pb_3(PO_4)_2$ and amorphous $Pb_3P_2O_8$ were subjected to five cycles of deep discharge and charge between 0.005 and 1.4 V (versus Li) at the rate of 30 mA/g. The charge capacities and Coulombic efficiencies as a function of the cycle number are shown in Fig. 3. For crystalline $Pb_3(PO_4)_2$, the charge capacity decreases dramatically from 742 mAh/g in the first cycle to 329 mAh/g in the second cycle. This lower value of charge capacity is almost preserved in the next three cycles, as shown in Fig. 3. The amorphous $Pb_3P_2O_8$ also undergoes a similar capacity fade, but the second cycle charge capacity of 350 mAh/g, though a substantial reduction from the initial charge capacity of 568 mAh/g, is a higher figure than the 329 mAh/g from crystalline $Pb_3(PO_4)_2$. A comparison of the two curves in Fig. 3 shows the main advantages of amorphous $Pb_3P_2O_8$: namely higher and more consistent charge and discharge capacities, and higher Coulombic efficiencies from the first to the fifth cycle relative to crystalline $Pb_3(PO_4)_2$.

Reactions between lithium and metal oxides at high temperatures (400°C) and at room temperature have been previously investigated [4,5]. It is generally agreed that the reactions progress sequentially in steps: the first step is the reductive decomposition of the metal oxide by Li to form lithium oxide and metal in the zero-valent state. This is then followed by an alloying reaction between Li and the reduced metal

$$(2y - x)\mathrm{Li} + \mathrm{Li}_x\mathrm{MO}_y \rightarrow y\mathrm{Li}_2\mathrm{O} + \mathrm{M} \quad (x \geq 0) \tag{1}$$

$$x\mathrm{Li} + \mathrm{M} + \mathrm{e}^- \rightarrow \mathrm{Li}_x\mathrm{M} \tag{2}$$

Similar reactions may also occur in a rechargeable lithium battery, as have been verified by Dahn and co-workers for the TCO anodes [6]. Reversibility of the second reaction is the key to cell rechargeability and the viability of the TCO system is based on the presence of facile inter-conversions between Li_xSn alloys of different compositions. An analogous situation may also prevail in the Li–Pb system. From the ex situ XRD patterns of $Pb_3(PO_4)_2$ charged to 5 mV and discharged to 1.4 V, it was found that the crystallinity of starting $Pb_3(PO_4)_2$ was completely destroyed after one charging cycle. The situation is similar to the obliteration of the XRD patterns of crystalline SnO_2 electrodes after insertion with different amounts of lithium [7]. Typically, with the increase in the extent of lithium insertion, the intensities of the characteristic peaks of crystalline SnO_2 diminish slowly to zero, indicating the gradual destruction of the SnO_2 lattice. The peak intensities from the remains of metallic lead and Li–Pb alloys between $2\theta = 25$ and 60° are generally weak and indistinct. This is good indication of the inadequate aggregation of lead atoms to form domains that are large enough for coherent X-ray diffraction.

A two-step charge transfer reaction may perhaps be proposed for lithium insertion into crystalline $Pb_3(PO_4)_2$ (Fig. 2a). The first step is related to the destruction of crystallinity of starting $Pb_3(PO_4)_2$. The material becomes amorphous in terms of long-range structural order but it may not be identical to amorphous $Pb_3P_2O_8$ in terms of site energetics and voltammetric response. Irrespective of the crystallinity of starting $Pb_3P_2O_8$, the lead atoms dispersed in the Li_3PO_4 network are the hosts for further Li insertion to form Li–Pb alloys. The opposite reaction of de-alloying occurs during discharge. A schematic representation of the reactions is given below only for heuristic purpose. Evaluations on the long-term stability of the material, which depends on the effectiveness of the lithium phosphate matrix to cushion the volume change during insertion and extraction of lithium, are currently in the work.

$$6\mathrm{Li}^+ + \mathrm{Pb}_3(\mathrm{PO}_4)_2 + 6\mathrm{e}^- \rightarrow 3\mathrm{Pb} + 2\mathrm{Li}_3\mathrm{PO}_4 \tag{3}$$

$$x\mathrm{Li}^+ + \mathrm{Pb} + x\mathrm{e}^- \rightarrow \mathrm{Li}_x\mathrm{Pb} \tag{4}$$

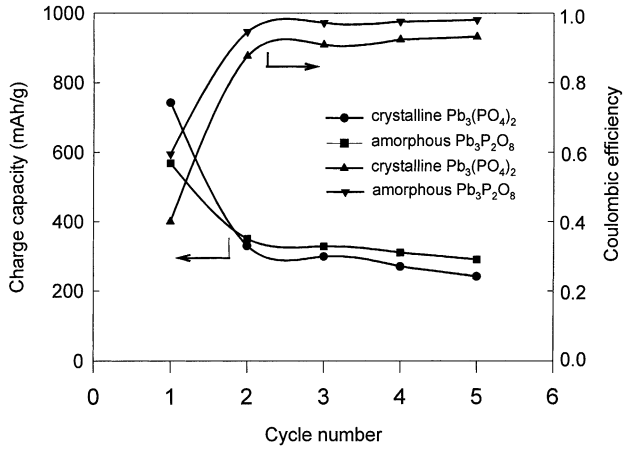

Fig. 3. Variation in charge capacity and Coulombic efficiency with cycle number.

4. Conclusions

Amorphous $Pb_3P_2O_8$ could be obtained from crystalline $Pb_3(PO_4)_2$ through a simple melt-quenching procedure.

Both crystalline $Pb_3(PO_4)_2$ and amorphous $Pb_3P_2O_8$ are capable of reversible Li^+ insertion and extraction in the potential range of 0–1.4 V. Higher charge and discharge

capacities, and more consistent cycling performance are obtained from the amorphous form.

The XRD patterns of crystalline $Pb_3(PO_4)_2$ and amorphous $Pb_3P_2O_8$ after one complete cycle of charge and discharge are similar, indicating that similar reaction products are formed and similar alloying mechanisms are involved for electrochemical energy storage and withdrawal.

Acknowledgements

The authors would like to acknowledge Ms. Ruifen Zhang for experimental assistance.

References

[1] J. Wang, P. King, R.A. Huggins, Solid State Ionics 20 (1986) 185.
[2] Y. Idota, M. Nishima, Y. Miyaki, T. Kubota, T. Miyasaki, Canada Patent Appl. 2,134,053 (1994).
[3] I.A. Courtey, J.R. Dhan, J. Electrochem. Soc. 144 (1997) 2045.
[4] N.A. Godshall, I.D. Raistrick, R.A. Huggins, Mater. Res. Bull. 15 (1980) 561.
[5] H. Li, X. Huang, L. Chen, Solid State Ionics 123 (1999) 189.
[6] I.A. Courtey, J.R. Dhan, J. Electrochem. Soc. 144 (1997) 2943.
[7] W. Liu, X. Huang, Z. Wang, H. Li, L. Chen, J. Electrochem. Soc. 145 (1998) 59.